

## ***Ab initio* calculation of the Hubbard $U$ and Hund exchange $J$ in local moment magnets: The case of Mn-based full Heusler compounds**

M. Tas <sup>1,\*</sup>, E. Şaşıoğlu <sup>2,†</sup>, S. Blügel <sup>3</sup>, I. Mertig <sup>2</sup>, and I. Galanakis <sup>4,‡</sup>

<sup>1</sup>*Department of Physics, Gebze Technical University, 41400 Kocaeli, Turkey*

<sup>2</sup>*Institute of Physics, Martin Luther University Halle-Wittenberg, 06120 Halle (Saale), Germany*

<sup>3</sup>*Peter Grünberg Institut and Institute for Advanced Simulation, Forschungszentrum Julich and JARA, 52425 Julich, Germany*

<sup>4</sup>*Department of Materials Science, School of Natural Sciences, University of Patras, GR-26504 Patra, Greece*



(Received 25 October 2021; revised 12 September 2022; accepted 21 October 2022; published 2 November 2022)

Mn-based full Heusler compounds possess well-defined local atomic Mn moments, and thus the correlation effects between localized  $d$  electrons are expected to play an important role in determining the electronic and magnetic properties of these materials. Employing *ab initio* calculations in conjunction with the constrained random-phase approximation (cRPA) method, we calculate the strength of the effective on-site Coulomb interaction parameters (Hubbard  $U$  and Hund exchange  $J$ ) in the case of  $X_2MnZ$  full Heusler compounds with  $X$  being one of Ni, Pd, or Cu, and  $Z$  being one of In, Sn, Sb, or Te. We show that the  $Z$  element (or  $sp$  element) in Heusler compounds significantly reduces the strength of the Hubbard  $U$  parameter for Mn  $3d$  electrons compared to the elementary bulk Mn. On the contrary, the effect of the  $sp$  atom on the strength of the  $U$  parameter of Ni, Cu, or Pd valence  $d$  electrons is not so substantial with respect to the elementary bulk values. The  $U$  values for all transition-metal atoms decrease with increasing  $sp$  electron numbers in the In-Sn-Sb-Te sequence. Our cRPA calculations reveal that despite their well-defined local magnetic moments, the Mn-based full Heusler alloys fall into the category of the weakly correlated materials.

DOI: [10.1103/PhysRevMaterials.6.114401](https://doi.org/10.1103/PhysRevMaterials.6.114401)

### I. INTRODUCTION

$Cu_2MnAl$ , the prototype Heusler compound, was synthesized more than a century ago [1,2]. Since this initial discovery, hundreds of compounds and alloys crystallizing in similar lattices have been grown experimentally [3,4]. Due to their large number and variety of the chemical elements, which can act as constituents, Heusler compounds and alloys present a richness of physical phenomena [3–5]. Already in the 60s, full Heusler compounds with chemical formula  $X_2MnZ$ —where  $X$  is Ni, Pd, or Cu, and  $Z$  is In, Sn or Sb—were grown in the  $L2_1$  lattice structure and were studied for their magnetic properties [6–8]. These compounds are often characterized as best metallic local moment magnets since the spin magnetic moment is concentrated and localized at the Mn atoms, and the long range Mn-Mn exchange interactions determine the magnetic behavior [9–11]. The interest on these Heusler compounds has been intensified recently since it was shown that the off-stoichiometric Heusler alloys containing Ni and Mn may present a martensitic phase transition which is accompanied by strong magneto-caloric effects [12–15]. This class of materials is well-known in literature as ferromagnetic shape memory alloys [16–20]. Magnetic Heusler compounds and alloys are also promising materials for the rapidly growing fields of magnetoelectronics and spintronics [21]. Several

aspects of the  $(Ni, Pd, Cu)_2Mn(In, Sn, Sb)$  Heusler compounds have been studied recently including the nature of the exchange interactions [10,11], spinwaves [22,23], electronic properties [24–26], the spin polarization [27], and the martensitic phase transition [28,29].

Although electronic band structure calculations based on the density functional theory (DFT) are quite successful in the study of magnetic systems, the presence of  $3d$  and  $4d$  transition-metal atoms in the local moment magnetic Heusler compounds means that the electronic correlations may play an important role in the determination of their electronic and magnetic properties. For example, it was shown in Ref. [23] for the compounds  $Ni_2MnSn$  and  $Pd_2MnSn$  that the electronic correlations play a crucial role in correct determination of the spin-waves spectra. Also as shown by Shourov and collaborators in the case of  $FeVSb$ , a semiconducting Heusler compound, the inclusion of on-site correlations in the calculations leads to an enhancement of the effective electron mass by 40% in agreement with their experimental findings [30].

There are two common ways to include the correlations in the first-principles electronic structure calculations. The first one is the so-called  $LDA+U$  or  $GGA+U$  ( $LDA$  acronym stands for “local density approximation”, and  $GGA$  for “generalized gradient approximation”) scheme where an effective on-site Coulomb repulsion term Hubbard  $U$  and Hund exchange  $J$  are used to account for the correlation effects [31,32]. This approach has been proven to be accurate in the case of transition-metal oxides [31,32]. But the  $LDA+U$  and  $GGA+U$  schemes are not suitable for metallic systems

\*murat.tas@gtu.edu.tr

†ersoy.sasioglu@physik.uni-halle.de

‡galanakis@upatras.gr

and they cannot describe the nonquasiparticle states in half metallic Heusler compounds [33]. A more elaborate modern computational scheme, which has resulted from merging of the DFT and many-body Hamiltonian methods, is the so-called LDA+DMFT where DMFT stands for dynamical mean field theory [34,35]. The LDA+DMFT schemes have been proven to be successful in determining the electronic properties of  $3d$  ferromagnets and several extensions also including the nonlocal correlations which have been proposed [36]. Except LDA, the GGA functional has also been used in conjunction with the DMFT method, and thus in the following when we use the term LDA+DMFT, we also imply the GGA+DMFT scheme.

Determination of the Coulomb interaction parameters (Hubbard  $U$  and Hund exchange  $J$ ) from experimental data is a very difficult task and only scarce data exists. Thus, it is highly desirable to directly calculate these parameters, which are materials specific, from the first principles [37–39]. The earliest approach is the wellknown constrained local-density approximation (cLDA) [40–42]. The cLDA is still in wide use even though it is known to deliver unreasonably large  $U$  and  $J$  values especially for the late transition-metal atoms due to the difficulties in compensating for the self-screening error of localized electrons [41]. Moreover, since the Hubbard  $U$ , within the cLDA approach, is calculated in the framework of DFT, frequency dependence of the  $U$  cannot be obtained. Contrary to cLDA, the constrained random-phase approximation (cRPA) does not suffer from these deficiencies and allows individual Coulomb matrix elements to be accessed—e.g., on-site, off-site, intra-orbital, inter-orbital, and exchange elements—including their frequency dependence [43–51]. The cRPA method has been applied to a variety of material classes including elementary transition-metal atoms [31,47,49], half-metallic Heusler compounds [52],  $f$ -electron systems [53], double perovskites [54], oxides [31] and transition-metal oxides, and perovskites [44,49]. Here, we should note that the actual  $U$  value used in the LDA+DMFT calculations depends on the adopted low-energy model and may need to be considerably increased with respect to its calculated value [55].

Motivated by the interest on the local moment magnets, we aim in the present work to determine the strength of the Coulomb interaction parameters (Hubbard  $U$  and Hund exchange  $J$ ) using the cRPA method for twelve Mn-based  $X_2MnZ$  ( $X = \text{Ni, Cu, Pd, and } Z = \text{In, Sn, Sb, Te}$ ) full Heusler compounds. This study provides a complete picture on the behavior of the Coulomb interaction parameters in local moment Mn-based Heusler magnets upon variation of both  $X$  and  $Z$  atoms. Our calculations have shown that the  $Z$  atoms play an essential role in determining the strength of the effective Coulomb interaction between  $3d$  electrons of Mn atoms in these materials. Specifically, strength of the  $U$  for Mn- $3d$  electrons is substantially reduced with respect to the corresponding value in bulk Mn. Moreover, the  $U$  value decreases with increasing  $sp$ -electron numbers in the In-Sn-Sb-Te sequence. The rest of the paper is organized as follows: in Sec. II we present details of our calculations, in Sec. III we present and discuss our results, and in Sec. IV we summarize and conclude.

## II. COMPUTATIONAL METHODOLOGY

In this section we will briefly discuss the method for calculating the effective Coulomb interaction parameters for the Mn-based Heusler compounds by providing references to previous articles where the methodology is presented in detail.

The compounds with  $Z$  being In, Sn, or Sb are well known to grow in the so-called  $L2_1$  cubic lattice of the Heusler compounds; the lattice is a fcc with four atoms along the diagonal as basis with Wyckoff positions:  $X = (0\ 0\ 0)$ ,  $Mn = (\frac{1}{4}\ \frac{1}{4}\ \frac{1}{4})$ ,  $X = (\frac{1}{2}\ \frac{1}{2}\ \frac{1}{2})$ , and  $Z = (\frac{3}{4}\ \frac{3}{4}\ \frac{3}{4})$  [6–8]. The compounds with Te atoms have not been grown yet experimentally, but we include them for reasons of completeness. In Table I we include the lattice constants used in the calculations which are the equilibrium lattice constants determined through the total energy calculations. For all compounds, the lattice constant exceeds 6 Å and for the same  $Z$  atom it increases in the sequence Ni-Cu-Pd.

The ground-state calculations for all studied full Heusler compounds were carried out using the full-potential linearized augmented plane waves (FLAPW) method as implemented in the FLEUR code [56] within the GGA of the exchange-correlation potential as parametrized by Perdew, Burke, and Ernzerhof (PBE) [57]. Note that due to the metallic character of the compounds under study, the GGA provides a more accurate description of the ground state properties with respect to more complex hybrid functionals [58]. For all calculations we used angular momentum and plane-wave cutoff parameters of  $l_{\max} = 10$  inside the spheres, and  $k_{\max} = 4.5a_B^{-1}$  for the outside region. The DFT-PBE calculations were performed using a  $20 \times 20 \times 20$   $\mathbf{k}$ -point grid in the Brillouin zone. For compounds including In atoms, FLEUR uses local orbitals for semi-core  $4d$  states.

The maximally localized Wannier functions (MLWFs) were constructed with the WANNIER90 code [59–63]. The effective Coulomb potential was calculated within the cRPA method [43–45] implemented in the SPEX code [64] (for further technical details see Ref. [65]). We used a  $8 \times 8 \times 8$   $\mathbf{k}$ -point grid, and 500 unoccupied bands in the cRPA calculations. We also performed test calculations with a  $6 \times 6 \times 6$   $\mathbf{k}$ -point grid; the difference in the calculated parameters was of the order of 0.01 eV in most cases compared to the more dense case. In full Heusler compounds, the Mn- $3d$  states are strongly hybridized with the Ni- $3d$  (Cu- $3d$ , Pd- $4d$ ) states as well as with the  $5p$  states of the  $Z$  atom as revealed by the density of states (DOS) plots presented for the case of Ni-compounds in Fig. 1 (the bands corresponding to the Mn- $3d$  states scan the same energy window as the bands for the Ni- $3d$  states while a less pronounced overlap also exists with the  $Z$  valence  $p$  states). Thus we construct the Wannier functions for the  $3d$  ( $4d$ ) orbitals of the transition-metal atoms using at least 19 bands. In some parts of the Brillouin zone a few more states are included due to the mixing with other bands.

The chosen 15 Wannier orbitals well represent the correlated Hilbert space, for which in Fig. 2 we compare the Wannier-interpolated (WI) band structure with the DFT one, denoted as KS (Kohn-Sham), for the case of  $\text{Ni}_2\text{MnIn}$ . We see that the agreement for  $\text{Ni}_2\text{MnIn}$  is almost perfect. Figures S1-S3 in the Supplemental Material present a similar comparison for the other three studied compounds containing Ni

TABLE I. The lattice constants,  $d$  orbitals, average spread of the Wannier functions  $\Omega$ , bare (unscreened)  $V$  and  $J_b$ , partially screened Hubbard  $U$  and Hund exchange  $J$ ,  $U_{\text{eff}}$ , and fully screened on-site Coulomb interaction parameters  $\tilde{U}$  and  $\tilde{J}$  between the localized  $d$  orbitals in twelve Heusler compounds. In parenthesis we provide computed  $U$  and  $J$  values which are calculated by excluding  $5p$  screening channel of the Z atom (see text for a detailed discussion).

Compound	a (Å)	Orbital	$\Omega$ (Å <sup>2</sup> )	$V$ (eV)	$J_b$ (eV)	$U$ (eV)	$J$ (eV)	$U_{\text{eff}}$ (eV)	$\tilde{U}$ (eV)	$\tilde{J}$ (eV)
Ni <sub>2</sub> MnIn	6.08	Ni-3d	1.88	23.01	1.16	3.60 (5.58)	1.03 (1.06)	2.57	0.75	0.73
		Mn-3d	7.17	18.97	0.96	2.60 (5.48)	0.83 (0.88)	1.77	0.13	0.28
Ni <sub>2</sub> MnSn	6.02	Ni-3d	2.12	22.66	1.14	3.43 (4.70)	1.00 (1.02)	2.43	0.88	0.76
		Mn-3d	7.72	18.51	0.93	2.57 (4.62)	0.80 (0.85)	1.77	0.14	0.29
Ni <sub>2</sub> MnSb	6.00	Ni-3d	1.84	22.23	1.11	3.07 (3.77)	0.96 (0.97)	2.11	1.06	0.78
		Mn-3d	8.70	17.85	0.89	2.33 (3.57)	0.76 (0.79)	1.57	0.16	0.31
Ni <sub>2</sub> MnTe	6.07	Ni-3d	1.72	21.81	1.08	2.47 (2.65)	0.92 (0.92)	1.55	1.02	0.76
		Mn-3d	8.24	16.82	0.82	1.62 (1.96)	0.67 (0.69)	0.95	0.12	0.24
Pd <sub>2</sub> MnIn	6.37	Pd-3d	2.41	15.70	0.88	3.00 (4.79)	0.77 (0.82)	2.23	1.26	0.68
		Mn-3d	7.74	19.42	0.99	2.34 (6.12)	0.85 (0.94)	1.49	0.11	0.25
Pd <sub>2</sub> MnSn	6.38	Pd-3d	2.03	15.65	0.87	2.94 (4.29)	0.76 (0.80)	2.18	1.36	0.69
		Mn-3d	8.90	19.04	0.96	2.36 (5.28)	0.82 (0.90)	1.54	0.11	0.25
Pd <sub>2</sub> MnSb	6.42	Pd-3d	2.01	15.54	0.86	2.66 (3.32)	0.74 (0.75)	1.92	1.44	0.68
		Mn-3d	10.78	18.44	0.92	2.03 (3.80)	0.78 (0.83)	1.25	0.11	0.25
Pd <sub>2</sub> MnTe	6.35	Pd-3d	2.19	15.42	0.85	2.47 (2.66)	0.73 (0.73)	1.74	1.44	0.68
		Mn-3d	13.59	17.55	0.87	1.69 (2.20)	0.71 (0.74)	0.98	0.11	0.22
Cu <sub>2</sub> MnIn	6.19	Cu-3d	1.07	24.95	1.27	4.75 (6.81)	1.16 (1.23)	3.59	2.67	1.08
		Mn-3d	9.82	17.95	0.89	1.77 (4.23)	0.73 (0.91)	1.04	0.15	0.29
Cu <sub>2</sub> MnSn	6.20	Cu-3d	0.99	24.82	1.26	4.38 (5.63)	1.14 (1.19)	3.24	2.71	1.08
		Mn-3d	11.24	17.07	0.84	1.54 (3.01)	0.67 (0.78)	0.87	0.14	0.27
Cu <sub>2</sub> MnSb	6.10	Cu-3d	1.18	24.64	1.25	3.89 (4.82)	1.12 (1.17)	2.77	2.70	1.07
		Mn-3d	12.23	15.73	0.75	1.10 (1.83)	0.58 (0.69)	0.52	0.14	0.26
Cu <sub>2</sub> MnTe	6.27	Cu-3d	1.09	24.51	1.24	3.48 (4.34)	1.10 (1.15)	2.38	2.54	1.06
		Mn-3d	10.94	14.05	0.65	0.55 (1.23)	0.44 (0.62)	0.11	0.09	0.18

[66]. In their case, there are parts of the band structure where the Wannier-interpolated band structure deviates from the KS one due to the  $p$  admixture discussed above. Moreover, in the fourth column of Table I we present the average spread of the Wannier functions for all materials. The Wannier spreads provide qualitative information on the localization of the Wannier functions, which will be discussed in the following section. Note that, as shown in Ref. [67], the Wannier spreads do not correlate with the accuracy of the Wannier interpolation scheme. Finally, in the Supplemental Material we present the

center of all Wannier functions and their respective spreads for all compounds (see Tables S1-S12 in [66]).

In the cRPA approach, the full polarization matrix  $P$  is divided into two parts:  $P = P_d + P_r$ , where  $P_d$  includes only  $d$ - $d$  transitions and  $P_r$  is the remainder. Then, the frequency-dependent effective Coulomb interaction is given schematically by the matrix equation  $U(\omega) = [1 - vP_r(\omega)]^{-1}v$ , where  $v$  is the bare Coulomb interaction and  $U(\omega)$  is related to the fully screened interaction by  $\tilde{U}(\omega) = [1 - U(\omega)P_d(\omega)]^{-1}U(\omega)$ .

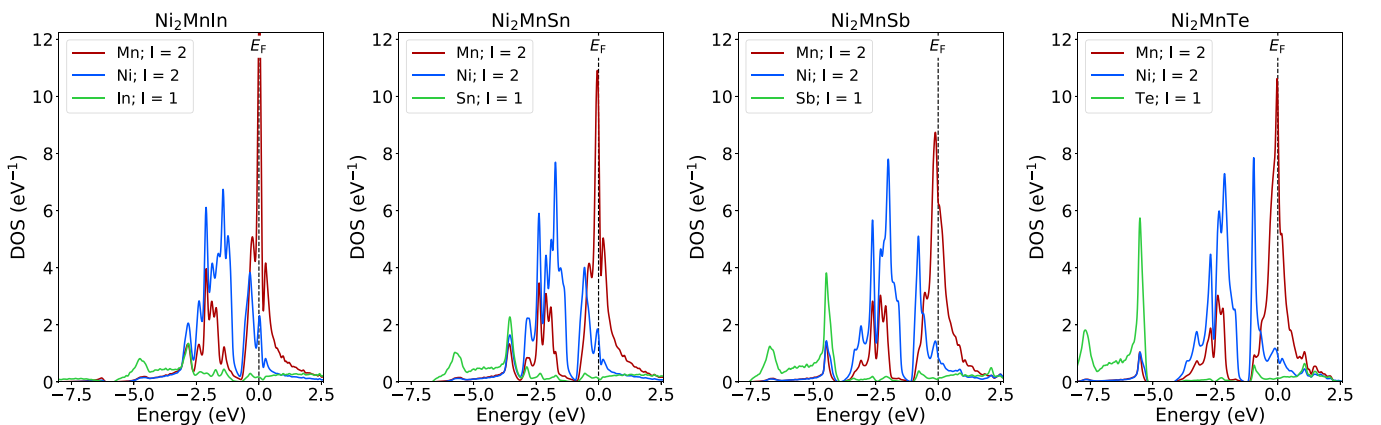


FIG. 1. Atom-resolved  $l$ -projected density of states (DOS) for nonmagnetic Ni<sub>2</sub>MnIn, Ni<sub>2</sub>MnSn, Ni<sub>2</sub>MnSb, and Ni<sub>2</sub>MnTe. For all compounds the Fermi level is set to zero energy.

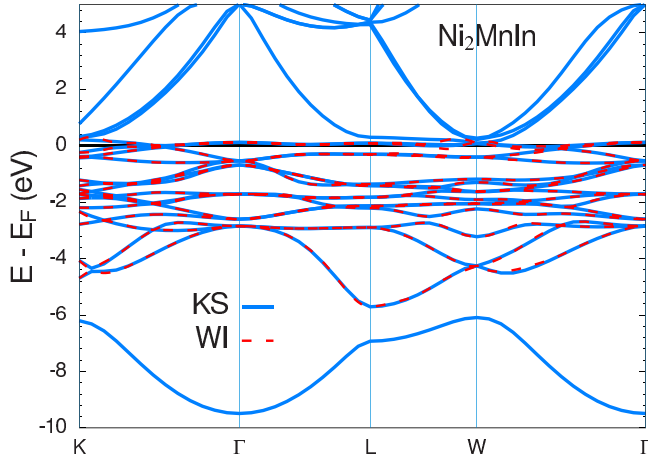


FIG. 2. Comparison of the DFT (KS) and the Wannier-interpolated (WI) band structures of  $\text{Ni}_2\text{MnIn}$  along the high symmetry lines in the Brillouin zone.

We consider matrix elements of  $U$  in the MLWF basis

$$U_{in_1, jn_3, in_2, jn_4}(\omega) = \iint d\mathbf{r}d\mathbf{r}' w_{in_1}^*(\mathbf{r})w_{jn_3}^*(\mathbf{r}')U(\mathbf{r}, \mathbf{r}', \omega)w_{jn_4}(\mathbf{r}')w_{in_2}(\mathbf{r}). \quad (1)$$

In the static limit ( $\omega \rightarrow 0$ ) the so-called Slater parametrization of the Coulomb matrix is given by

$$U = \frac{1}{L^2} \sum_{m,n} U_{mn;mn} = F^0, \quad (2)$$

$$J = U - \frac{1}{L(L-1)} \sum_{m \neq n} [U_{mn;mn} - U_{nm;nm}] \quad (3)$$

$$= (F^2 + F^4)/14, \quad (4)$$

where  $L$  is the number of localized orbitals, i.e., five for  $d$  orbitals,  $F^0$ ,  $F^2$ , and  $F^4$  are the Slater integrals. Similar to  $U$  and  $J$ , we can also define so-called fully screened  $\tilde{U}$  and  $\tilde{J}$  parameters as well as unscreened (or bare)  $V$  and  $J_b$  parameters. Although the fully screened Coulomb interaction parameters are not used in model Hamiltonians, they provide an idea about the correlation strength of considered electrons.

### III. RESULTS AND DISCUSSIONS

As mentioned in the preceding section, due to the strong hybridization of Mn- $3d$  states with Ni- $3d$  (Pd- $4d$ , Cu- $3d$ ) as well as the  $5p$  states of the Z atom, all twelve Heusler compounds can be described by an effective fifteen-orbital low-energy model, five  $3d$  orbitals stemming from the Mn atom, and ten  $3d$  ( $4d$ ) orbitals stemming from the Ni, Cu (Pd) atoms. Note that in the model Hamiltonian description of the Heusler compounds, the noninteracting one-body part of the effective model is defined for a nonmagnetic state, and thus calculation of the effective Coulomb interaction parameters should be based on the same state. In the following, we will discuss the effective Coulomb interaction parameters calculated within the cRPA method considering the Slater

parametrization of the Coulomb matrix for the nonmagnetic state.

In Table I we present all computed results for all twelve compounds studied. The calculations are material specific, and for each compound we provide computed values of the bare (unscreened) Coulomb interaction parameters  $V$ ,  $J_b$ , partially screened (Hubbard  $U$ , Hund exchange  $J$ ) as well as fully screened interaction parameters for both X and Mn atoms. In the nonmagnetic case, the  $V$  parameters provide information on extension (or spread  $\Omega$ ) of the Wannier functions, while as for the fully screened Coulomb interaction parameters of the Mn atom one should not attribute a physical meaning to them due to the strong change of electronic structure, i.e., sharp Mn- $3d$  peaks around the Fermi level (see Fig. 1), which gives rise to a strong screening. In the ferromagnetic case of all these compounds, one can obtain larger fully screened Coulomb interaction parameters for the Mn atom due to the large exchange splitting of the Mn- $3d$  states. On the other hand, for the X atoms we expect similar parameters in the magnetic and nonmagnetic cases since the exchange splitting is negligibly small for these atoms, especially in the case of Cu-based compounds. In the following, the fully screened Coulomb interaction parameters will not be discussed as they are presented purely for the sake of completeness.

For  $3d$  elements, the bare  $V$  Coulomb interaction increases with increasing  $d$ -electron numbers, in agreement with previous calculations. In the case of In-based compounds,  $V$  varies from 19 eV for the Mn atom to 25 eV for the Cu atoms and this behavior can be attributed to the localization of the Wannier functions with increasing nuclear charge. An increase in the nuclear charge causes the  $3d$  wave functions to contract, which gives rise to the observed trend for  $V$  and  $J_b$ . As we move within the same column of the periodic table from  $3d$  to  $4d$  elements, i.e., from Ni to Pd, the  $V$  value decreases due to the more delocalized character of the  $4d$  Wannier functions of the Pd atom. For all compounds, the Wannier functions are slightly delocalized as we move from In to Te, which is reflected in the calculated spreads and bare Coulomb interaction parameters presented in Table I. For instance, in the case of Ni-based compounds, the  $V$  for Ni- $3d$  electrons decreases from 23 eV to 21.8 eV, while for the Mn- $3d$  electrons this reduction is slightly larger, from 19 eV to 16.8 eV.

We now would like to discuss the calculated Hubbard  $U$  parameters. Obtained  $U$  parameters for X atoms in the In- and Sn-based compounds are more or less comparable to the corresponding values in the elementary transition metals presented in Refs. [31,47,49]. With increasing  $sp$ -electron numbers, i.e., along the In-Sn-Sb-Te sequence, the  $U$  values for the X atoms decrease substantially, especially in the case of Cu- and Ni-based compounds. As discussed above, this reduction partially stems from the delocalization of the Wannier functions, but the main contribution comes from the complex screening effects. Screening increases with increasing  $sp$ -electron numbers, and thus results in smaller Coulomb interaction parameters. The same discussion also holds for the effective Coulomb interaction parameter of Mn- $3d$  electrons. However the computed  $U$  values are significantly smaller than the corresponding value in elementary Mn atoms, which can be attributed to the efficient screening of  $sp$  elements (Z atoms) in Heusler compounds.

Finally, we discuss relative values of the on-site Coulomb interactions  $U$  and of the width  $W$  of the  $d$ -bands. The ratio  $U/W$  determines whether the material is a weakly or a strongly correlated system. The situation is similar to the elementary  $3d$  transition metals [47] and the half-metallic Heusler compounds [52]. Occupied  $d$ -states, as shown in Fig. 1, scan an energy window  $W$  of about 4–6 eV width, depending on the specific Ni-based material. The  $U$  values for the Ni and Mn atoms in these compounds (presented in Table I) are smaller than  $W$ , which means that the  $U/W$  ratio is smaller than one and these materials are characterized as weakly correlated materials, similar to the elementary  $3d$  transition metals [47] and the half-metallic Heusler compounds [52]. The same arguments also stand for the Pd- and Cu-based compounds under study. Note that, similar to the studies in Refs. [47] and [52], the  $U$  values do not differ significantly between the  $e_g$  and  $t_{2g}$  states; in Sec. I of the Supplemental Material [66], we present, as an example, the  $U_{mn;mn}$  values used in Eq. 2 for the  $3d$  orbitals of Ni and Mn atoms in the  $\text{Ni}_2\text{MnIn}$  compound.

To reveal the contribution of the  $sp$  element ( $Z$  atom) to screening of the effective Coulomb interaction parameters, we present, in Table I inside the parenthesis, the  $U$  values calculated with excluding the  $Z$  atom  $5p$  screening channel. That is, in the computation of the polarization function (see Ref. [47] for technical details) in addition to the exclusion of the  $3d \rightarrow 3d$  (or  $3d \rightarrow 3d$  and  $3d \rightarrow 4d$  in Pd-based compounds) transitions we also exclude the  $3d \rightarrow 5p$  ( $3d \rightarrow 5p$  and  $4d \rightarrow 5p$ ) transitions. As is seen, the  $Z$  atom  $5p$  screening channel provides a significant contribution to the strength of the Hubbard  $U$  parameter in Heusler compounds. The obtained  $U$  values with and without the  $5p$  screening channel differ more than by a factor of two in some cases, especially in the case of In- and Sn-based compounds. In these two cases, the  $5p$  channel is less than half filled and provides a substantial contribution to the screening process. In the case of Te-based compounds, the  $5p$  channel is more than half filled and thus, its contribution is reduced significantly.

Up to now, we have discussed the strength of the effective Coulomb interaction parameter  $U$  in Heusler compounds. Unlike the  $U$  parameter, the Hund exchange  $J$  is much less screened, as the screening of the exchange interaction is monopolelike in contrast to dipolelike screening of the  $U$  parameter (see Ref. [46] for a detailed discussion). Thus, the value of the Hund exchange  $J$  is close to the corresponding unscreened atomic value (see Table I). Note that our computed  $J$  values are larger than the ones presented in Refs. [47,52] for the elementary transition metals and half metallic Heusler compounds. This difference is due to the different parametrization of the Coulomb matrix since in those two cited papers the Hubbard-Kanamori parametrization is employed instead of the Slater parametrization in the present work.

In Table I, we also present the  $U_{\text{eff}} = U - J$ , which is the so-called effective Hubbard  $U$ .  $U_{\text{eff}}$  is used in Dudarev's approach which is a simplified implementation of the DFT+ $U$  method [68–71]. This approach, in conjunction with GGA, was employed in Ref. [23] where the spin-wave spectra of  $\text{Ni}_2\text{MnSn}$  and  $\text{Pd}_2\text{MnSn}$  have been calculated. There, an arbitrary  $U_{\text{eff}}$  value of 1.5 eV for the Mn- $3d$  orbitals was considered. This value is very close to our calculated

TABLE II. Off-site (intersublattice) effective Coulomb interaction parameters in eV.  $X$  stands for Ni, Pd, or Cu depending on the chemical type of the compound. We should note that Mn- $X$  are the nearest neighbors while Mn-Mn and  $X$ - $X$  are the next-nearest neighbors.

$X_2\text{Mn}Z$	$U_{\text{Mn}-X}$ (eV)	$U_{X-X}$ (eV)	$U_{\text{Mn}-\text{Mn}}$ (eV)
$\text{Ni}_2\text{MnIn}$	0.47	0.38	0.19
$\text{Ni}_2\text{MnSn}$	0.49	0.39	0.20
$\text{Ni}_2\text{MnSb}$	0.44	0.35	0.18
$\text{Ni}_2\text{MnTe}$	0.24	0.19	0.08
$\text{Pd}_2\text{MnIn}$	0.36	0.31	0.13
$\text{Pd}_2\text{MnSn}$	0.40	0.33	0.15
$\text{Pd}_2\text{MnSb}$	0.29	0.23	0.09
$\text{Pd}_2\text{MnTe}$	0.25	0.20	0.08
$\text{Cu}_2\text{MnIn}$	0.39	0.31	0.16
$\text{Cu}_2\text{MnSn}$	0.32	0.25	0.11
$\text{Cu}_2\text{MnSb}$	0.20	0.14	0.07
$\text{Cu}_2\text{MnTe}$	0.09	0.07	0.03

effective Hubbard  $U_{\text{eff}}$  values for the Mn- $3d$  states shown in Table I (1.54 eV for  $\text{Pd}_2\text{MnSn}$  and 1.77 eV for  $\text{Ni}_2\text{MnSn}$ ). It was found that GGA+ $U$  was a considerable improvement over usual GGA calculations in reproducing the experimental spectra with accuracy, stressing the importance of accurate determination of the Coulomb parameters.

In Table II, we again present the Coulomb interaction parameters, but now the off-site ones between  $d$  orbitals of neighboring atoms are included in the table. These values, as expected, are one order of magnitude smaller than the on-site Coulomb interaction parameters discussed just above. The exact values depend not only on the chemical elements themselves but also on the distance between neighboring atoms, and localization of the Wannier functions. The Mn- $X$  atoms are the nearest neighbors while the Mn-Mn and  $X$ - $X$  pairs of atoms are the next nearest neighbors, and this explains the larger values in the first column. As we move from one compound to another, we cannot identify a very clear trend since variation of the off-site  $U$  value seems to depend on both the lattice constant and chemical elements. It is considerably smaller when the  $Z$  atom is Te. Although one may conclude that the off-site Coulomb repulsion terms can be neglected when the Hubbard-type model Hamiltonians are used to describe electronic band structure, such a statement is an oversimplification since its validity depends on the studied properties. The importance of the off-site Coulomb interactions for certain properties (for example, the ones related to charge transfer) is enhanced due to the connectivity of the lattice and the long-range  $1/r$ -tail of the partially screened Coulomb interaction present in the cRPA treatment [72–74], and these parameters might be necessary for an accurate modeling of these materials.

Finally we would like to discuss the frequency dependence of the effective Coulomb interaction parameter  $U$  by considering the Ni-based compounds. In Fig. 3, we plot both the real (positive values) and imaginary (negative values) parts of the Coulomb interaction parameter  $U$  as a function of the frequency  $\omega$ . The  $U$  values presented in Table I are the static limit of the real part when the frequency tends to zero. For the Hubbard model to be accurate, the  $U$  values near the

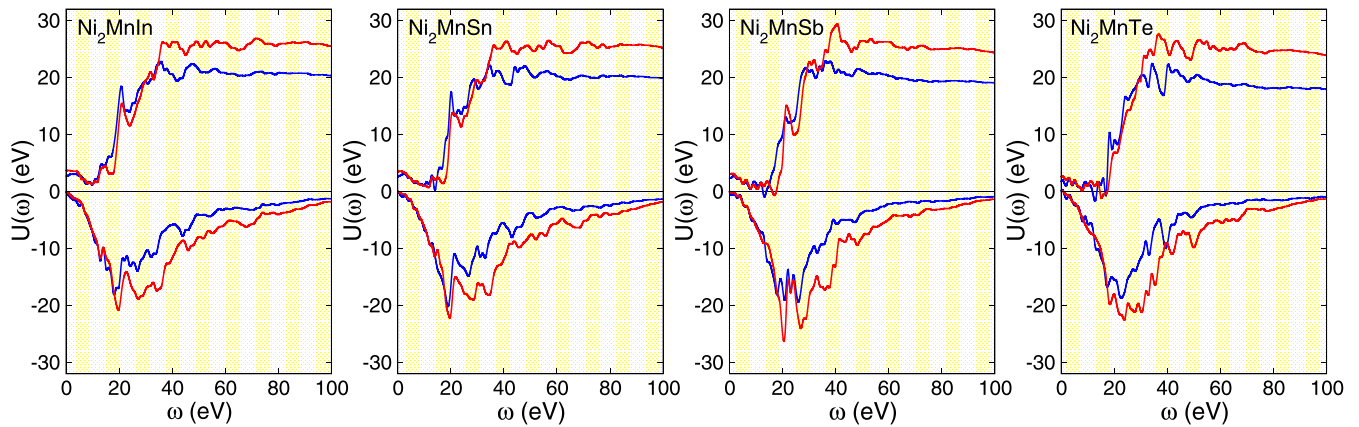


FIG. 3. Real (positive values) and imaginary (negative values) part of the calculated on-site Coulomb interaction  $U$  as a function of the frequency  $\omega$  for the Ni (red) and Mn (blue) atoms in the nonmagnetic  $\text{Ni}_2\text{MnIn}$ ,  $\text{Ni}_2\text{MnSn}$ ,  $\text{Ni}_2\text{MnSb}$ , and  $\text{Ni}_2\text{MnTe}$  compounds.

zero frequency should be quite stable as was the case in the half-metallic Heusler compounds [52]. This is not the case in the compounds under study. With the exception of  $\text{Ni}_2\text{MnIn}$ , as we move away from the zero frequency,  $U$  vanishes at the plasmon frequency and then shows an abrupt increase reaching the bare  $V$  value which remains almost constant for large  $\omega$  values. Exactly at the plasmon frequency the imaginary part of  $U$  exhibits the first large peak and its value is around 20–25 eV for all four Ni-based compounds in Fig. 3. Thus, we expect that the static Hubbard models like the LDA+ $U$  and GGA+ $U$  methods might not be so accurate in describing their electronic and magnetic structure of these compounds. We should also mention that we have also investigated behavior of the Hund exchange  $J$  parameter as a function of  $\omega$ . The  $J$  is not sensitive to  $\omega$ , and its value remains almost constant for all considered frequency values (in all cases it shows a very small increase of less than 0.1 eV at the plasmon frequency and then remains constant).

#### IV. CONCLUSIONS

Employing the cRPA method within the FLAPW framework we have calculated the strength of the on-site Coulomb interaction parameters (Hubbard  $U$  and Hund exchange  $J$ ) between the localized  $d$ -electrons in  $\text{X}_2\text{MnZ}$  ( $X = \text{Ni, Pd, Cu}$ ;  $Z = \text{In, Sn, Sb, Te}$ ) Heusler compounds, which are known to be best local moment magnets. Our calculations have shown that due to the presence of the  $Z$  element (or  $sp$  element) in Heusler compounds, the strength of the Hubbard  $U$  parameter

for the Mn  $3d$  electrons is significantly reduced compared to the elementary bulk Mn. In the case of the  $d$  electrons of Ni, Cu, and Pd, the strength difference of the  $U$  parameter between the studied Heusler compounds and the elementary bulk Ni, Cu, or Pd is not so substantial. Moreover, the  $U$  values for the transition metal valence  $d$  electrons decrease with increasing  $sp$  electron numbers in the In-Sn-Sb-Te sequence. The calculated off-site Coulomb parameters are one order of magnitude smaller than the on-site ones. Frequency dependent calculations of the  $U$  parameter reveal that the static limit might not be a good approximation for these compounds, with the exception of the ones containing In.

Our cRPA calculations reveal that, despite their well-defined local magnetic moments, the Mn-based full Heusler alloys fall into the category of the weakly correlated materials. Knowledge of the Coulomb interaction parameters plays an important role in the construction of model Hamiltonians aiming to study the correlation effects in electronic structure of ternary magnetic compounds. We expect that our study will enhance the interest in Heusler compounds which are local moment magnets.

#### ACKNOWLEDGMENTS

E.Ş. and I.M. acknowledge support from Sonderforschungsbereich TRR 227 of the Deutsche Forschungsgemeinschaft (DFG) and funding provided by the European Union (EFRE), Grant No. ZS/2016/06/79307. Authors thank Christoph Friedrich for fruitful and helpful discussions.

- [1] F. Heusler, Verh. Dtsch. Phys. Ges. **5**, 219 (1903).
- [2] F. Heusler and E. Take, Phys. Z. **13**, 897 (1912).
- [3] P. J. Webster and K. R. A. Ziebeck, in *Alloys and Compounds of d-Elements with Main Group Elements. Part 2.*, edited by H. R. J. Wijn, Landolt-Börnstein, New Series, Group III, Vol. 19, Pt.c (Springer-Verlag, Berlin 1988), pp. 75–184.
- [4] K. R. A. Ziebeck and K.-U. Neumann, in *Magnetic Properties of Metals*, edited by H. R. J. Wijn, Landolt-Börnstein, New Series, Group III, Springer, Berlin (2001), Vol. 32/c, pp. 64–414.

- [5] T. Graf, C. Felser, and S. S. P. Parkin, *Prog. Solid State Chem.* **39**, 1 (2011).
- [6] D. P. Oxley, R. S. Tebble, C. T. Slack, and K. C. Williams, *Nature (London)* **194**, 465 (1962).
- [7] P. J. Webster and R. S. Tebble, *J. Appl. Phys.* **39**, 471 (1968).
- [8] P. J. Webster, *Contemp. Phys.* **10**, 559 (1969).
- [9] J. Kübler, A. R. Williams, and C. B. Sommers, *Phys. Rev. B* **28**, 1745 (1983).

- [10] E. Şaşıoğlu, L. M. Sandratskii, and P. Bruno, *Phys. Rev. B* **70**, 024427 (2004).
- [11] E. Şaşıoğlu, L. M. Sandratskii, and P. Bruno, *Phys. Rev. B* **77**, 064417 (2008).
- [12] V. D. Buchelnikov, P. Entel, S. V. Taskaev, V. V. Sokolovskiy, A. Hucht, M. Ogura, H. Akai, M. E. Gruner, and S. K. Nayak, *Phys. Rev. B* **78**, 184427 (2008).
- [13] V. V. Sokolovskiy, V. D. Buchelnikov, M. A. Zagrebin, P. Entel, S. Sahoo, and M. Ogura, *Phys. Rev. B* **86**, 134418 (2012).
- [14] D. Comtesse, M. E. Gruner, M. Ogura, V. V. Sokolovskiy, V. D. Buchelnikov, A. Grünebohm, R. Arróyave, N. Singh, T. Gottschall, O. Gutfleisch, V. A. Chernenko, F. Albertini, S. Fähler, and P. Entel, *Phys. Rev. B* **89**, 184403 (2014).
- [15] V. V. Sokolovskiy, M. E. Gruner, P. Entel, M. Acet, A. Çakır, D. R. Baigutlin, and V. D. Buchelnikov, *Phys. Rev. Mater.* **3**, 084413 (2019).
- [16] Y. Sutou, Y. Imano, N. Koeda, T. Omori, R. Kainuma, K. Ishida, and K. Oikawa, *Appl. Phys. Lett.* **85**, 4358 (2004).
- [17] X. Moya, L. Mañosa, A. Planes, T. Krenke, M. Acet, and E. F. Wassermann, *Mater. Sci. Eng. A* **438–440**, 911 (2006).
- [18] L. Mañosa, X. Moya, A. Planes, S. Aksoy, M. Acet, E. F. Wassermann, and T. Krenke, *Mater. Sci. Forum* **583**, 111 (2008).
- [19] A. Planes, L. Mañosa, and M. Acet, *J. Phys.: Condens. Matter* **21**, 233201 (2009).
- [20] T. Krenke, M. Acet, E. F. Wassermann, X. Moya, L. Mañosa, and A. Planes, *Phys. Rev. B* **72**, 014412 (2005).
- [21] K. Elphick, W. Frost, M. Samiepour, T. Kubota, K. Takanashi, H. Sukegawa, S. Mitani, and A. Hirohata, *Sci. Technol. Adv. Mater.* **22**, 235 (2021).
- [22] I. Galanakis and E. Şaşıoğlu, *J. Mater. Sci.* **47**, 7678 (2012).
- [23] G. Fischer, X. Zubizarreta, A. Marmodoro, M. Hoffmann, P. Buczek, N. Buczek, M. Däne, W. Hergert, E. Şaşıoğlu, I. Galanakis, and A. Ernst, *Phys. Rev. Mater.* **4**, 064405 (2020).
- [24] S. K. Bose, J. Kudrnovský, V. Drchal, and I. Turek, *Phys. Rev. B* **82**, 174402 (2010).
- [25] F. Aguilera-Granja, R. H. Aguilera-del-Toro, and J. L. Morán-López, *Mater. Res. Express* **6**, 106118 (2019).
- [26] B. Hamri, B. Abbar, A. Hamri, O. Baraka, A. Hallouche, and A. Zaoui, *Comput. Condens. Matter* **3**, 14 (2015).
- [27] M. Obaida, L. Galdun, T. Ryba, V. Komanicky, K. Saksl, M. Durisin, J. Kovac, V. Haskova, P. Szabo, Z. Vargova, and R. Varga, *Intermetallics* **85**, 139 (2017).
- [28] S. Pramanick, P. Dutta, J. Sannigrahi, K. Mandal, S. Bandyopadhyay, S. Majumdar, and S. Chatterjee, *J. Phys.: Condens. Matter* **30**, 405803 (2018).
- [29] W. Wang, S.-S. Gao, and Y. Meng, *J. Magn. Magn. Mater.* **371**, 135 (2014).
- [30] E. H. Shourov, P. J. Strohbeen, D. Du, A. Sharan, F. C. de Lima, F. Rodolakis, J. L. McChesney, V. Yannello, A. Janotti, T. Biroli, and J. K. Kawasaki, *Phys. Rev. B* **103**, 045134 (2021).
- [31] K. Karlsson, F. Aryasetiawan, and O. Jepsen, *Phys. Rev. B* **81**, 245113 (2010).
- [32] I. V. Solovyev, *J. Phys.: Condens. Matter* **20**, 293201 (2008).
- [33] M. I. Katsnelson, V. Yu. Irkhin, L. Chioncel, A. I. Lichtenstein, and R. A. de Groot, *Rev. Mod. Phys.* **80**, 315 (2008).
- [34] J. Minár, *J. Phys.: Condens. Matter* **23**, 253201 (2011).
- [35] F. Lechermann, A. Georges, A. Poteryaev, S. Biermann, M. Posternak, A. Yamasaki, and O. K. Andersen, *Phys. Rev. B* **74**, 125120 (2006).
- [36] G. Rohringer, H. Hafermann, A. Toschi, A. A. Katanin, A. E. Antipov, M. I. Katsnelson, A. I. Lichtenstein, A. N. Rubtsov, and K. Held, *Rev. Mod. Phys.* **90**, 025003 (2018).
- [37] T. Kotani, *J. Phys.: Condens. Matter* **12**, 2413 (2000).
- [38] I. V. Solovyev and M. Imada, *Phys. Rev. B* **71**, 045103 (2005).
- [39] I. Schnell, G. Czucholl, and R. C. Albers, *Phys. Rev. B* **65**, 075103 (2002).
- [40] P. H. Dederichs, S. Blügel, R. Zeller, and H. Akai, *Phys. Rev. Lett.* **53**, 2512 (1984).
- [41] V. I. Anisimov and O. Gunnarsson, *Phys. Rev. B* **43**, 7570 (1991); M. Cococcioni and S. de Gironcoli, *ibid.* **71**, 035105 (2005).
- [42] K. Nakamura, R. Arita, Y. Yoshimoto, and S. Tsuneyuki, *Phys. Rev. B* **74**, 235113 (2006).
- [43] F. Aryasetiawan, M. Imada, A. Georges, G. Kotliar, S. Biermann, and A. I. Lichtenstein, *Phys. Rev. B* **70**, 195104 (2004).
- [44] F. Aryasetiawan, K. Karlsson, O. Jepsen, and U. Schönberger, *Phys. Rev. B* **74**, 125106 (2006).
- [45] T. Miyake, F. Aryasetiawan, and M. Imada, *Phys. Rev. B* **80**, 155134 (2009).
- [46] T. Miyake and F. Aryasetiawan, *Phys. Rev. B* **77**, 085122 (2008).
- [47] E. Şaşıoğlu, C. Friedrich, and S. Blügel, *Phys. Rev. B* **83**, 121101(R) (2011).
- [48] T. O. Wehling, E. Şaşıoğlu, C. Friedrich, A. I. Lichtenstein, M. I. Katsnelson, and S. Blügel, *Phys. Rev. Lett.* **106**, 236805 (2011).
- [49] B.-C. Shih, Y. Zhang, W. Zhang, and P. Zhang, *Phys. Rev. B* **85**, 045132 (2012); B.-C. Shih, T. A. Abtew, X. Yuan, W. Zhang, and P. Zhang, *ibid.* **86**, 165124 (2012).
- [50] H. Sims, W. H. Butler, M. Richter, K. Koepf, E. Şaşıoğlu, C. Friedrich, and S. Blügel, *Phys. Rev. B* **86**, 174422 (2012).
- [51] Y. Nomura, M. Kaltak, K. Nakamura, C. Taranto, S. Sakai, A. Toschi, R. Arita, K. Held, G. Kresse, and M. Imada, *Phys. Rev. B* **86**, 085117 (2012); Y. Nomura, K. Nakamura, and R. Arita, *ibid.* **85**, 155452 (2012).
- [52] E. Şaşıoğlu, I. Galanakis, C. Friedrich, and S. Blügel, *Phys. Rev. B* **88**, 134402 (2013).
- [53] F. Nilsson, R. Sakuma, and F. Aryasetiawan, *Phys. Rev. B* **88**, 125123 (2013).
- [54] A. Neroni, E. Şaşıoğlu, H. Hadipour, C. Friedrich, S. Blügel, I. Mertig, and M. Ležaić, *Phys. Rev. B* **100**, 115113 (2019).
- [55] M. Casula, Ph. Werner, L. Vaugier, F. Aryasetiawan, T. Miyake, A. J. Millis, and S. Biermann, *Phys. Rev. Lett.* **109**, 126408 (2012).
- [56] <http://www.flapw.de>
- [57] J. P. Perdew, K. Burke, and M. Ernzerhof, *Phys. Rev. Lett.* **77**, 3865 (1996).
- [58] M. Meinert, *Phys. Rev. B* **87**, 045103 (2013).
- [59] N. Marzari and D. Vanderbilt, *Phys. Rev. B* **56**, 12847 (1997).
- [60] A. A. Mostofi, J. R. Yates, Y.-S. Lee, I. Souza, D. Vanderbilt, and N. Marzari, *Comput. Phys. Commun.* **178**, 685 (2008).
- [61] A. A. Mostofi, J. R. Yates, G. Pizzi, Y. S. Lee, I. Souza, D. Vanderbilt, and N. Marzari, *Comput. Phys. Commun.* **185**, 2309 (2014).

- [62] I. Souza, N. Marzari, and D. Vanderbilt, *Phys. Rev. B* **65**, 035109 (2001).
- [63] F. Freimuth, Y. Mokrousov, D. Wortmann, S. Heinze, and S. Blügel, *Phys. Rev. B* **78**, 035120 (2008).
- [64] C. Friedrich, S. Blügel, and A. Schindlmayr, *Phys. Rev. B* **81**, 125102 (2010).
- [65] E. Şaşıoğlu, A. Schindlmayr, C. Friedrich, F. Freimuth, and S. Blügel, *Phys. Rev. B* **81**, 054434 (2010).
- [66] See Supplemental Material at <http://link.aps.org/supplemental/10.1103/PhysRevMaterials.6.114401> for more detailed information regarding the  $U$  matrix elements, the band structures and the details of the interpolated Wannier functions.
- [67] K. F. Garrity and K. Choudhary, *Sci. Data* **8**, 106 (2021).
- [68] S. L. Dudarev, G. A. Botton, S. Y. Savrasov, C. J. Humphreys, and A. P. Sutton, *Phys. Rev. B* **57**, 1505 (1998).
- [69] P. Baettig, C. Ederer, and N. A. Spaldin, *Phys. Rev. B* **72**, 214105 (2005).
- [70] V. I. Anisimov, F. Aryasetiawan, and A. I. Lichtenstein, *J. Phys.: Condens. Matter* **9**, 767 (1997).
- [71] V. I. Anisimov, I. V. Solovyev, M. A. Korotin, M. T. Czyzyk, and G. A. Sawatzky, *Phys. Rev. B* **48**, 16929 (1993).
- [72] M. Schüler, M. Rösner, T. O. Wehling, A. I. Lichtenstein, and M. I. Katsnelson, *Phys. Rev. Lett.* **111**, 036601 (2013).
- [73] T. P. Hansmann, T. Ayrat, L. Vaugier, P. Werner, and S. Biermann, *Phys. Rev. Lett.* **110**, 166401 (2013).
- [74] P. Seth, O. E. Peil, L. Pourovskii, M. Betzinger, C. Friedrich, O. Parcollet, S. Biermann, F. Aryasetiawan, and A. Georges, *Phys. Rev. B* **96**, 205139 (2017).